

# How magic is the magic $^{68}\text{Ni}$ nucleus?

K. Langanke<sup>1,2</sup>, J. Terasaki<sup>2-4</sup>, F. Nowacki<sup>5</sup>, D.J. Dean<sup>2</sup>, and W. Nazarewicz<sup>2,3,6</sup>

<sup>1</sup>*Institute of Physics and Astronomy, University of Aarhus, DK-8000 Aarhus C, Denmark*

<sup>2</sup>*Physics Division, Oak Ridge National Laboratory, Oak Ridge, TN 37831 USA*

<sup>3</sup>*Department of Physics, University of Tennessee, Knoxville, TN 37996, USA*

<sup>4</sup>*Joint Institute for Heavy Ion Research, Oak Ridge National Laboratory, Oak Ridge, TN 37831 USA*

<sup>5</sup>*Institut de Recherches Subatomiques, IN2P3-CNRS-Université Louis Pasteur, F-67037 Strasbourg Cedex 2, France*

<sup>6</sup>*Institute for Theoretical Physics, University of Warsaw, ul. Hoża 69, PL-00-681, Warsaw, Poland*

(November 30, 2018)

We calculate the  $B(E2)$  strength in  $^{68}\text{Ni}$  and other nickel isotopes using several theoretical approaches. We find that in  $^{68}\text{Ni}$  the gamma transition to the first  $2^+$  state exhausts only a fraction of the total  $B(E2)$  strength, which is mainly collected in excited states around 5 MeV. This effect is sensitive to the energy splitting between the  $fp$  shell and the  $g_{9/2}$  orbital. We argue that the small experimental  $B(E2)$  value is not strong evidence for the double-magic character of  $^{68}\text{Ni}$ .

The appearance of shell gaps associated with magic nucleon numbers is one of the cornerstones of nuclear structure. The presence of magic gaps allows one, for example, to determine the single-particle energies and the residual interaction among valence nucleons, providing essential input for nuclear models. Magic gaps offer a natural way of performing truncations in microscopic many-body calculations. Magic nuclei also play an essential role in the two major nucleosynthesis networks (s- and r-process) that produce the majority of nuclides heavier than mass number  $A \sim 60$ .

The doubly-magic character of  $^{68}\text{Ni}$  ( $Z=28$ ,  $N=40$ ) was suggested in the early eighties [1,2] and tested experimentally [4–7]. The proton number  $Z=28$  in the nickel isotopes is magic. In the neutrons, the sizeable energy gap at  $N=40$  separates the  $pf$  spherical shell from the  $g_{9/2}$  intruder orbit. However, this spherical subshell closure is not sufficiently large to stabilize the spherical shape. [Experimentally [3],  $^{80}\text{Zr}$  ( $N=Z=40$ ) behaves like a well-deformed rotor.] The current experimental evidence about the double-magicity of  $^{68}\text{Ni}$  is controversial [8]. On the one hand,  $^{68}\text{Ni}$  does not show a pronounced irregularity in the two-neutron separation energies, as is expected for a magic nucleus. On the other hand, the lowered position of the  $0_2^+$  level, the slightly elevated energy of the first  $2^+$  state, and the quite small  $B(E2, 0_{\text{g.s.}}^+ \rightarrow 2_1^+)$  value are often interpreted as indications for magicity. In fact, the  $B(E2)$  rate in  $^{68}\text{Ni}$  ( $280 \pm 60 \text{ e}^2\text{fm}^4$  [7]) is significantly smaller than that in the well-established double-magic nucleus  $^{56}\text{Ni}$  ( $620 \pm 120 \text{ e}^2\text{fm}^4$  [9]).

As discussed in Ref. [10], the size of the  $N=40$  gap strongly depends on the effective interaction used, and it dramatically influences the quadrupole collectivity of the  $N=40$  nuclei. While there is much discussion in the literature about the weakening of shell effects in neutron-rich nuclei (e.g., the magic gap  $N=28$  seems to be eroded in drip-line systems; see Ref. [10] and references quoted

therein),  $^{68}\text{Ni}$  lies very far from the expected neutron drip line (expected to be around  $^{92}\text{Ni}$  [11]) and one should probably not invoke “exotic” explanations when discussing the structure of this neutron rich nucleus.

It is the aim of this Letter to draw attention to the total  $B(E2; 0_{\text{g.s.}}^+ \rightarrow 2_f^+)$  distribution in  $^{68}\text{Ni}$ , which can hold the key to the question whether this nucleus is magic or not. We will argue that the transition to the first excited  $2^+$  state constitutes only a small part of the total  $B(E2)$  strength and that the total  $B(E2)$  strength depends sensitively on the size of the  $N=40$  shell gap.

To understand the structural difference between  $^{68}\text{Ni}$  and  $^{56}\text{Ni}$  (where the transition to the first  $2^+$  state exhausts most of the total low-energy strength), we begin from qualitative arguments based on a simple independent particle model (IPM). Proton configurations in both nuclei are identical and correspond to a closed ( $f_{7/2}$ ) shell. The neutron configuration in  $^{56}\text{Ni}$  is the same as the proton one, ( $f_{7/2}$ )<sup>8</sup>, while in  $^{68}\text{Ni}$  it corresponds to the closed ( $pf$ ) shell. The first excited  $2^+$  state can be viewed as a superposition of particle-hole (ph) excitations. In  $^{56}\text{Ni}$ , the lowest proton and neutron ph excitations are identical (due to isospin symmetry) and they are of (1p-1h) character. The  $2_1^+$  state can be roughly expressed as  $1/\sqrt{2}(\Phi_p(1p-1h) + \Phi_n(1p-1h))$ . Due to the parity change between ( $pf$ ) and  $g_{9/2}$  orbits, the  $2_1^+$  state in  $^{68}\text{Ni}$  cannot have a 1p-1h neutron component. It can thus be written as  $\alpha\Phi_p(1p-1h) + \beta\Phi_n(2p-2h)$ , where  $|\alpha|^2 + |\beta|^2 = 1$ . The weight  $|\beta|^2$  of the neutron component decreases with the size of the  $N=40$  gap. As  $B(E2)$  transitions reflect a proton component in the wave function, an increasing value of  $\beta$  reduces the  $B(E2)$  rate. Consequently, a smaller  $B(E2, 0_{\text{g.s.}}^+ \rightarrow 2_1^+)$  value in  $^{68}\text{Ni}$  than in  $^{56}\text{Ni}$  suggests that  $|\alpha|$  is noticeably smaller than  $1/\sqrt{2}$ , implying that it is more favorable in  $^{68}\text{Ni}$  to excite the pair of neutrons into the  $g_{9/2}$  orbital than to excite a single proton across the magic  $N=28$  gap. As the proton configurations in the  $^{56}\text{Ni}$  and  $^{68}\text{Ni}$  ground states are

the same, the IPM also suggests that a noticeable part of the (1p-1h) proton excitations in  $^{68}\text{Ni}$  should be mixed into excited states. Of course, the neutron amplitude  $|\beta|$ , hence the  $B(E2)$  rate, should also depend on the residual interaction. Therefore, to check whether the simple IPM argument also holds in the presence of a realistic residual interaction, we performed calculations in three different theoretical models: the Shell Model Monte Carlo (SMMC), the Quasi-particle Random-Phase Approximation (QRPA), and a large-scale diagonalization shell model (SM).

The SMMC approach allows the calculation of nuclear properties as thermal averages, employing the Hubbard-Stratonovich transformation to rewrite the two-body parts of the residual interaction by integrals over fluctuating auxiliary fields [12]. We performed SMMC studies of the even-even nickel isotopes between  $^{56}\text{Ni}$  and  $^{78}\text{Ni}$  in the complete ( $fp$ )( $gds$ ) configuration space for both protons and neutrons. The single-particle energies were derived from a Woods-Saxon potential appropriate for  $^{56}\text{Ni}$ , placing the important levels at excitation energies (in MeV) of 4.3 ( $p_{3/2}$ ), 6.4 ( $f_{5/2}$ ), 6.6 ( $p_{1/2}$ ), 9.0 ( $g_{9/2}$ ), 13.0 ( $d_{5/2}$ ) relative to the  $f_{7/2}$  orbital. We employed the same residual interaction of the type pairing-plus-quadrupole as in Ref. [15], which allowed us to avoid the sign problem in SMMC calculations [13]. We checked that our interaction gives a reasonable description of the collective spectrum of  $^{64}\text{Ge}$  and  $^{64}\text{Ni}$ , and that center-of-mass contaminations are small and do not affect our results for quadrupole excitations. The SMMC calculations were performed at temperature  $T=0.33$  MeV (corresponding to 96  $\Delta\beta$  ‘time slices’), which, for even-even nuclei, is sufficiently low to cool the nucleus to the ground state. We checked this for  $^{68}\text{Ni}$  and found variations of the various quadrupole expectation values of less than 3% by slightly increasing the temperature to  $T=0.4$  MeV. The Monte Carlo integrations used between 1000 and 4000 samples.

In the SMMC approach, the total  $B(E2)$  strength is approximated by the expectation value  $B(E2) \propto \langle \hat{Q}^2 \rangle$ , where the quadrupole operator is defined by  $\hat{Q} = e_p \hat{Q}_p + e_n \hat{Q}_n$ , with  $\hat{Q}_{p(n)} = \sum_i r_i^2 Y_2(\theta_i, \phi_i)$ ; the sum runs over all valence protons (neutrons). The effective charges  $e_p, e_n$  account for coupling to the states outside our model space. We adopt in the following the standard values  $e_p = 1.5, e_n = 0.5$  [14]. For the single-particle wave functions, we adopt the harmonic oscillator states with the oscillator length  $b = 1.01A^{1/6}$  fm. At low temperatures, the total  $B(E2)$  strength obtained in SMMC approximates the expectation value  $\langle 0_{\text{g.s.}}^+ | \hat{Q}^2 | 0_{\text{g.s.}}^+ \rangle = \sum_f |\langle 0_{\text{g.s.}}^+ | \hat{Q} | 2_f^+ \rangle|^2 \propto \sum_f B(E2; 0_{\text{g.s.}}^+ \rightarrow 2_f^+)$ . Therefore, the total SMMC strength corresponds to the *summed*  $B(E2)$  strength to the excited  $2^+$  states within the assumed configuration space.

The total SMMC  $B(E2)$  strengths are plotted in Fig. 1.

They follow the experimental transition rates rather

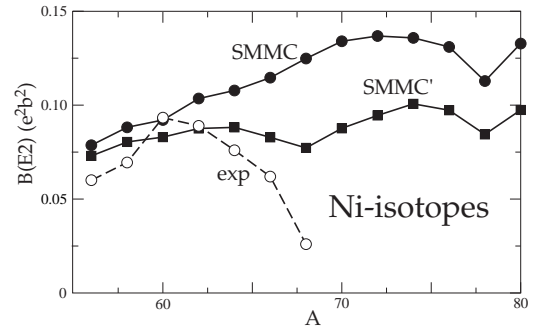


FIG. 1. Comparison of the total SMMC  $B(E2)$  values for even-even nickel isotopes (solid circles) with the experimental  $B(E2, 0_{\text{g.s.}}^+ \rightarrow 2_1^+)$  rates (open circles, from Ref. [16]). The solid squares represent the SMMC  $B(E2)$  values obtained in the SMMC' variant of calculations in which all the  $gds$  single-particle energies are shifted up by 1 MeV.

closely up to  $^{62}\text{Ni}$ . For these nuclei, it is well known from electron scattering experiments that most of the  $B(E2)$  strength resides in the transition to the first  $2^+$  state (see, e.g., Ref. [17]). For the isotopes approaching  $N = 40$ , SMMC predicts a significantly larger total  $B(E2)$  strength than observed in the first transition. For  $^{68}\text{Ni}$ , the calculated total strength ( $\sim 1250e^2\text{fm}^4$ ) is about five times greater than the measured transition to the first  $2^+$  state. This is consistent with the fact that the centroid of the SMMC  $B(E2)$  strength, calculated from the respective response function, lies at  $\sim 5$  MeV. This value is significantly higher than the energy of the first  $2^+$  state and indicates that most of the calculated SMMC  $B(E2)$  strength in  $^{68}\text{Ni}$  resides in excited states.

In Ref. [7] it was pointed out that the neutron  $g_{9/2}$  orbital plays a major role at  $N = 40$ , thanks to cross-shell neutron pairing excitations. We confirm this finding. In our SMMC study we find an average occupation number  $\langle n \rangle = 2.2$  for neutrons in the  $g_{9/2}$  orbital (and 0.22 in the  $d_{5/2}$  orbital which couples strongly to  $g_{9/2}$  by the quadrupole force). These numbers are significantly reduced (to 0.9 and 0.08, respectively) if one artificially shifts upwards all levels of the  $gds$  shell by 1 MeV, making the  $N=40$  gap larger (see the SMMC' variant of calculations in Fig. 1). As a consequence, the quadrupole moment of the neutron configuration gets reduced and the summed  $B(E2)$  value decreases. Although in this modified calculation the summed  $B(E2)$  value is smaller for  $^{68}\text{Ni}$  than in the neighboring nuclei, our calculation still predicts most of the strength in excited states. We note that for both sets of single-particle energies,  $^{78}\text{Ni}$  is characterized as magic, having a reduced  $B(E2)$  value compared to the neighbors. It is also worth mentioning that the variations of  $Q_p^2$  along the isotope chain are rather small. The smallest value is obtained for  $^{56}\text{Ni}$ , the

largest for  $^{72}\text{Ni}$ ; however, the variation is less than 9%. This shows again that proton ( $f_{7/2} \rightarrow p_{3/2}, p_{1/2}, f_{5/2}$ ) excitations cannot be neglected in the reproduction of the  $E2$  strength, as already noted in [7], but the dominating variations in the  $B(E2)$  strength come from the neutrons.

While the SMMC approach allows for the calculation of the summed strength in large model spaces, it is not capable of making detailed spectroscopic predictions. For this reason, we have also performed QRPA and diagonalization shell-model calculations. Our QRPA calculations closely follow the formalism described recently in Ref. [18]. As a residual two-body interaction, we use the sum of an isoscalar and an isovector quadrupole force, and a quadrupole pairing force. For the single-particle levels below the  $N$  ( $Z$ ) = 82 shell gap, we took those of the Woods-Saxon potential [20], and the unbound states were approximated by the Nilsson levels [21]. Guided by the experimental data (cf. Ref. [19]), the energy of the  $2p_{3/2}$  neutron state was shifted up by 1 MeV. For the strength of the isoscalar quadrupole force, we adopted the self-consistent value multiplied by 0.8, and for the isovector force we took  $\chi_{T=1} = -\frac{123.8}{A^{7/3}} [\frac{\text{MeV}}{\text{fm}^4}]$ . The renormalization factors of the pairing gaps are 0.8 (neutron) and 0.9 (proton). The bare charges are used for calculation of  $B(E2; 0^+ \rightarrow 2^+)$ , consistent with the large model space. The results are shown in Fig. 2.

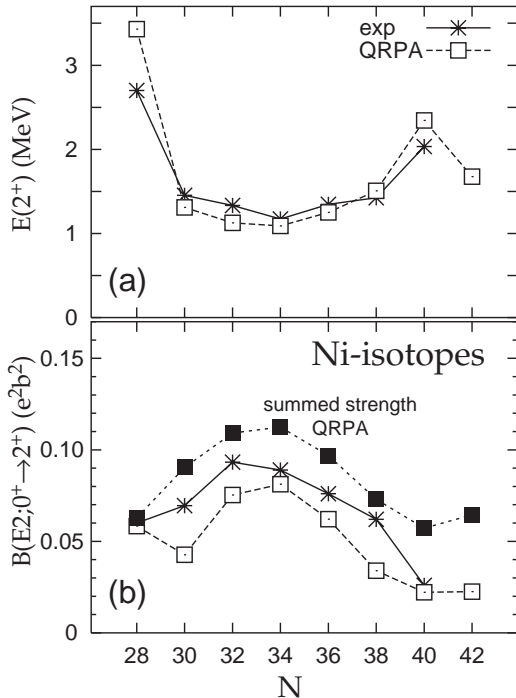


FIG. 2. (a) Comparison of the QRPA  $E_{2^+}$  energies and (b) summed  $B(E2)$  strength (filled squares) and  $B(E2, 0^+_{g.s.} \rightarrow 2^+)$  values with the experimental data. The summed  $B(E2)$  strength includes all the transitions up to an excitation energy of 9 MeV.

Our calculations nicely reproduce the observed trend of the  $E_{2^+}$  energies in Ni isotopes, including the pronounced rise at  $^{56}\text{Ni}$  and  $^{68}\text{Ni}$ . The QRPA calculations also give a reasonable description of the  $B(E2, 0^+_{g.s.} \rightarrow 2^+)$  values, with the maximum around  $^{62}\text{Ni}$  and the strong decrease towards  $^{68}\text{Ni}$ . The structure of the lowest  $2^+$  QRPA phonon in  $^{68}\text{Ni}$  is dominated by neutrons (90%). Importantly, our QRPA calculations confirm that most of the  $B(E2)$  strength in  $^{68}\text{Ni}$  resides in excited states, in contrast to  $^{56}\text{Ni}$ , where the  $B(E2)$  strength is exhausted by the transition to the first  $2^+$  state. These arguments are demonstrated again in Fig. 2, which displays the summed  $B(E2)$  strength (filled squares) and in Fig. 3, which shows the predicted  $B(E2)$  strength function. It is seen that around neutron number  $N = 40$ , a significant quadrupole strength develops at excitation energies around 4 MeV.

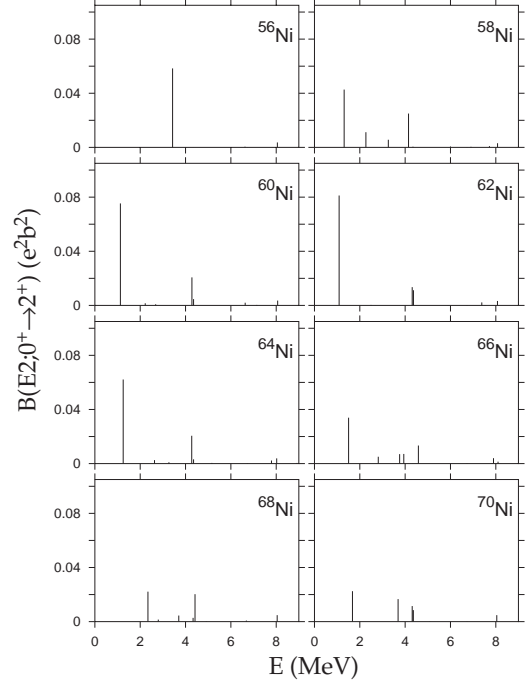


FIG. 3. Distribution of the  $B(E2; 0^+_{g.s.} \rightarrow 2^+)$  strength for even-even Ni isotopes calculated in the QRPA method.

Finally, our arguments have been tested and confirmed in large-scale diagonalization shell-model calculations of the  $B(E2)$  strength distribution in  $^{66,68}\text{Ni}$ . We adopt the same valence space and the effective interaction  $fpg$  employed in Ref. [7]. This valence space consists of a  $^{48}\text{Ca}$  core (more precisely, a  $^{40}\text{Ca}$  core with eight  $f_{7/2}$  frozen neutrons), the  $f_{7/2}$ ,  $p_{3/2}$ ,  $p_{1/2}$ , and  $f_{5/2}$  active orbitals for protons and the  $p_{3/2}$ ,  $p_{1/2}$ ,  $f_{5/2}$ , and  $g_{9/2}$  active orbitals for neutrons. The SM calculations describe well the behavior of the  $2^+$  energies and  $B(E2)$  rates for the Ni isotopes ranging from  $N=28$  to  $N=40$  [7]. The  $B(E2)$  strength distribution shown in Fig. 4 has been calculated

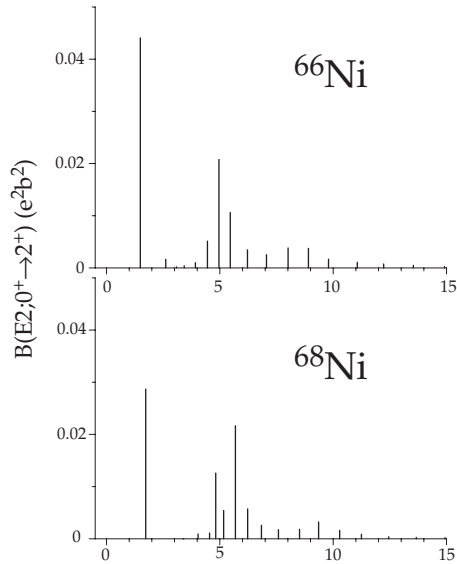


FIG. 4. Distribution of the  $B(E2; 0_{g.s.}^+ \rightarrow 2^+)$  strength in  $^{66,68}\text{Ni}$  calculated in the diagonalization shell model.

at a truncation level which considered up to a total of 7 particle excitations from the  $f_{7/2}$  orbital to the upper  $fp$  shell for protons and from the upper  $fp$  shell to the  $g_{9/2}$  orbital for neutrons. For  $^{68}\text{Ni}$ , the calculation predicts a  $B(E2)$  value of about  $280 \text{ e}^2\text{fm}^4$ , which nicely agrees with the experimental value. However, the transition to the first  $2^+$  state exhausts only the smaller fraction of the total shell-model  $B(E2)$  strength, which we calculate as  $900 \text{ e}^2\text{fm}^4$ . Most of the calculated strength resides at excitation energies around 5-6 MeV. The wave function of the first  $2_1^+$  state involves mainly (2p-2h) neutron excitations; the proton configuration is a mixture of 0p-0h (50%), 1p-1h ((25%), and 2p-2h (20%) components. The SM  $^{68}\text{Ni}$  ground state corresponds to a closed-shell configuration plus a 35% admixture of 2p-2h neutron excitations. The results for  $^{66}\text{Ni}$  nicely confirm the QRPA prediction: the transition strength is gradually shifted from the first excited state to higher energies as approaching  $N=40$ .

In summary, we have performed microscopic calculations of the  $B(E2; 0_{g.s.}^+ \rightarrow 2^+)$  strength distribution in  $^{68}\text{Ni}$ , and in other even-even nickel isotopes. Our main finding is that a significant portion of the  $B(E2)$  strength in  $^{68}\text{Ni}$  resides in excited states around 5 MeV, and that the small observed  $B(E2, 0_{g.s.}^+ \rightarrow 2_1^+)$  value is not necessarily an argument for a shell closure at  $N = 40$ . In fact, we argue that this transition rate is quite sensitive to the energy splitting between  $fp$  shell and  $g_{9/2}$  orbital, and that its smallness might indeed be an indication for a rather small gap. In short, the small  $B(E2)$  rate reflects the fact that the lowest  $2^+$  state in  $^{68}\text{Ni}$  is primarily a neutron excitation (cf. Ref. [18] for a similar discussion for  $^{136}\text{Te}$ ). If our arguments are correct, then most of

the  $B(E2)$  strength should reside in excited states. Further experimental investigations, including the  $g$ -factor measurement in  $^{68}\text{Ni}$ , are certainly called for.

## ACKNOWLEDGMENTS

We are indebted to Jonathan Engel for the use of his QRPA code. This work was supported in part by the U.S. Department of Energy under Contract Nos. DE-FG02-96ER40963 (University of Tennessee), DE-AC05-00OR22725 with UT-Battelle, LLC (Oak Ridge National Laboratory), the National Science Foundation Contract No. 0124053 (U.S.-Japan Cooperative Science Award), and by the Danish Research Council. Computational resources were provided by the Center for Computational Sciences, ORNL, and the National Energy Research Scientific Computing Center, Berkeley.

- 
- [1] M. Bernas *et al.*, Phys. Lett. **113B**, 279 (1982).
  - [2] R.J. Lombard and D. Mas, Phys. Lett. **120B**, 23 (1983).
  - [3] C.J. Lister *et al.*, Phys. Rev. Lett. **59**, 1270 (1987).
  - [4] R. Grzywacz *et al.*, Phys. Rev. Lett. **81**, 766 (1998).
  - [5] W.F. Mueller *et al.*, Phys. Rev. C **61**, 054308 (2000).
  - [6] T. Ishii *et al.*, Eur. Phys. J. A **13**, 15 (2002).
  - [7] O. Sorlin *et al.*, Phys. Rev. Lett. **88**, 092501 (2002).
  - [8] H. Grawe and M. Lewitowicz, Nucl. Phys. A **693**, 116 (2001).
  - [9] G. Kraus *et al.*, Phys. Rev. Lett. **73**, 1773 (1994).
  - [10] P.-G. Reinhard *et al.*, Phys. Rev. C **60**, 014316 (1999).
  - [11] W. Nazarewicz *et al.*, Phys. Rev. C **53**, 740 (1996).
  - [12] S.E. Koonin, D.J. Dean, and K. Langanke, Phys. Rep. **278**, 2 (1997).
  - [13] G.H. Lang *et al.*, Phys. Rev. C **48**, 1518 (1993).
  - [14] E. Caurier *et al.*, Phys. Rev. C **50**, 225 (1994).
  - [15] D.J. Dean, K. Langanke, and J. Sampaio, Phys. Rev. C in print.
  - [16] S. Raman, C.W. Nestor Jr., and P. Tikkanen, At. Data Nucl. Data Tabl. **78**, 1 (2001).
  - [17] K. Langanke *et al.*, Phys. Rev. C **52**, 718 (1995).
  - [18] J. Terasaki *et al.*, Phys. Rev. C, in press; nucl-th/0208042.
  - [19] A. Bohr and B.R. Mottelson, *Nuclear Structure*, vol. I (Benjamin, New York, 1969).
  - [20] S. Ćwiok *et al.*, Comp. Phys. Comm. **46**, 379 (1987).
  - [21] S.G. Nilsson *et al.*, Nucl. Phys. A **131**, 1 (1969).